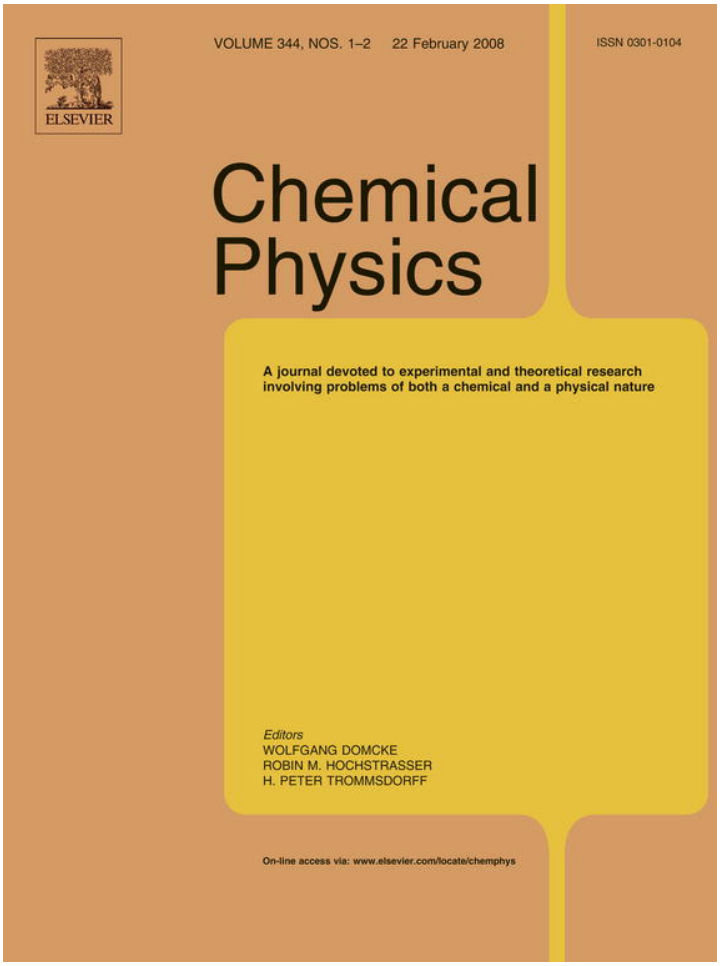

Available online at www.sciencedirect.com
ScienceDirect
Chemical Physics 344 (2008) 164–175
Chemical Physics
www.elsevier.com/locate/chemphys

VUV photophysics of acetonitrile: Fragmentation, fluorescence and ionization in the 7–22 eV region

Martin Schwell [a], Hans-Werner Jochims [b], Helmut Baumgärtel [b], Sydney Leach [c,*]

[a] *Laboratoire Interuniversitaire des Systèmes Atmosphériques (LISA), Université Paris 7 et 12, 61 Avenue du Général de Gaulle, 94010 Créteil Cedex, France*
[b] *Institut für Physikalische und Theoretische Chemie der Freien Universität Berlin, Takustr. 3, 14195 Berlin, Germany*
[c] *LERMA – UMR 8112, Observatoire de Paris-Meudon, 5, Place Jules Janssen, 92195 Meudon, France*

Received 19 September 2007; accepted 11 December 2007
Available online 23 December 2007

Abstract

VUV induced photodissociation of gaseous acetonitrile was studied in the 7–22 eV range using synchrotron radiation excitation, photofragment fluorescence spectroscopy and photoion mass spectrometry (PIMS). CN(A-X), CN(B-X) and CH(A-X) emissions were observed. Their relative intensities were studied by fluorescence excitation (FEX) spectroscopy. The fluorescence quantum yield for CN(B-X) emission is of the order of 1.5%, whereas that of CN(A-X) is of the order of 0.5%, relatively independent of excitation wavelength in the 9–20 eV region. The CN FEX spectra follow quite closely the photoabsorption spectrum. The total photoionization quantum yield of CH_3CN was measured up to 22 eV. The structures in the yield curve were related to photoabsorption features. The total photoionization quantum yield is about 0.5 at 13.131 eV, the energy of the first excited state of the ion; it reaches unity at about 21.3 eV. Dissociative reaction channels forming neutral products are discussed in detail. The results of this study and of an associated VUV absorption spectroscopy study of acetonitrile are used to discuss aspects of the interpretations of astrophysical observations of acetonitrile in the interstellar medium, comets and planetary atmospheres.

Keywords: Acetonitrile; VUV photophysics; Dissociative photoionization; Fragment fluorescence; Photoionization quantum yield; Astrophysical observations of acetonitrile

1. Introduction

Absorption of VUV photons by a polyatomic molecule, such as acetonitrile, can excite electronic and ionic states that give rise to many photophysical and photochemical relaxation processes. These include neutral dissociation, dissociative ionization and fluorescence of parent and/or fragment products [1]. Previous studies of the vacuum-UV (VUV) spectroscopy and photophysics of acetonitrile (CH_3CN) have been mainly limited to absorption and fluorescence measurements below 11.4 eV [2,3], apart from an absorption study [4] and a photoionization mass spectrometric study [5] up to 20 eV. VUV induced fluorescence, [3,6,7], was first observed by Neuimin and Terenin [8].

Acetonitrile, is considered to be a possible building block of biomolecules [9]. It has been observed in the interstellar medium [10–13], in comets [14,15], in the atmosphere of Titan [16,17] as well as in the Earth's stratosphere [18] and troposphere [19], which are all places where VUV and/or UV radiation is present. Knowledge of the VUV photophysics of acetonitrile is therefore useful for interpreting a number of astrophysical and atmospheric observations.

We have carried out extensive studies on the spectroscopy and photophysics of acetonitrile in the 7–22 eV energy region. An analysis of the 7–20 eV photoabsorption spectrum, involving four valence transitions, as well as a large number of Rydberg transitions to the ground and

* Corresponding author. Tel.: +33 1 4507 7561; fax: +33 1 4507 7100.
E-mail address: sydney.leach@obspm.fr (S. Leach).

0301-0104/$ - see front matter © 2007 Elsevier B.V. All rights reserved.
doi:10.1016/j.chemphys.2007.12.011

excited states of the acetonitrile cation, has been made and is published elsewhere [20]. In the present work we first present photofragment fluorescence spectra which provide insight into photoprocesses occurring in excited acetonitrile. The excitation energy dependence of the CH and CN emission features identified in the dispersed fluorescence spectra of CH_3CN was measured in a fluorescence excitation (FEX) spectral study over the photon excitation range 8–20 eV. Analysis of the FEX spectra is made with the aid of data from the VUV absorption spectra and thermochemical limit calculations of the relevant processes forming the emitting electronic states. In Table 1 are given the heats of formation at 298 K of the atomic or molecular species used to calculate thermochemical threshold energies of the various dissociation processes discussed in the present work. We have also measured, for the first time, the total photoionization quantum yield of acetonitrile between 11 and 22 eV and compared the photoionization yield curves with absorption and other spectra. The results of this study are used to discuss aspects of astrophysical observations involving this species. A brief preliminary report on this work has been given previously [21].

2. Experimental

Monochromatised synchrotron radiation was obtained from the Berlin electron storage ring BESSY I (multibunch mode) in association with a 1.5 m McPherson monochromator (Normal incidence (NIM), dispersion 5.6 Å/mm). The grating transmission function of the BESSY I monochromator is recorded by detecting the visible fluorescence emitted by the sodium salicylate layer placed on a quartz window. For fluorescence measurements, the synchrotron light beam is focused into an open brass cell, differentially pumped, containing acetonitrile vapor at a pressure typically around 10^{-3} mbar. Fluorescence induced in irradiated target molecules passes through a quartz window and is dispersed using a 20 cm focal length secondary monochromator (Jobin-Yvon H 20 UV, grating blazed at 300 nm). This monochromator has a fixed, exchangeable exit slit but has no entrance slit. The width of the effective "entrance slit" is given by the spatial extension of the exciting light beam (approximately 1 mm). The emitted fluorescence light, measured in the 250–700 nm wavelength range, is detected by a photon-counting Hamamatsu R6060 photomultiplier, cooled to 250 K by a Peltier element. The spectral response function of this arrangement has been determined by recording the spectrum emitted by a tungsten halogen lamp, which is then deconvoluted according to Planck's law. A dispersed fluorescence spectrum typically contains two points per nm. The resolution of these spectra is between 4 and 20 nm depending on the choice of the effective exit slit width.

Dispersed fluorescence measurements were carried out at several excitation energies between 10 and 16 eV. The excitation bandwidth was ≈0.8 nm. In recording the fluorescence excitation (FEX) spectra, the secondary monochromator is fixed at a desired wavelength with a large exit slit and the primary monochromator is tuned in steps of typically 50–100 meV (400–800 cm^{-1}). The FEX spectra are corrected for the grating transmission function of the primary monochromator and for the VUV photon flux, respectively. The bandwidth was ≈0.3 nm, and the FEX spectral resolution was 40 meV at 13 eV photon excitation energy. A high resolution VUV absorption spectrum of acetone was used for calibration of the observed FEX spectral wavelengths.

Total ionization quantum yields of acetonitrile were determined up to 22 eV, with measuring intervals of 10 meV, using the monochromatised synchrotron radiation source and a technique that we used previously for ionization yield measurements on polycyclic aromatic hydrocarbons, as discussed in detail elsewhere [22]. Commercial acetonitrile of highest available purity was used without further purification.

Table 1
Heats of formation (298 K) of species used to calculate thermochemical threshold energies

Species	Heat of formation (eV)	Reference
H	2.259	NIST [66]
$CH(X^2\Pi)$	6.157	NIST [66]
$CH(A^2\Delta)$	9.035	NIST [66] + HH [67]
$CH(B^2\Sigma^-)$	9.343	NIST [66] + HH [67]
$CN(X^2\Sigma^+)$	4.509	NIST [66]
$CN(A^2\Pi)$	5.640	NIST [66] + HH [67]
$CN(B^2\Sigma^+)$	7.708	NIST [66] + HH [67]
$HCN(X^1\Sigma^+)$	1.400	NIST [66]
$CH_3(1^2A_2'')$	1.513	NIST [66]
CH_2CN	2.539	LIAS [68]
$CH_3CN(1^1A_1)$	0.767	NIST [66]

3. Absorption spectroscopy of CH_3CN

We first briefly consider the absorption spectroscopy of this molecule (Figs. 1a, and 2), presented in detail elsewhere [20], as a necessary preliminary to a discussion of the results of our VUV photophysical study of acetonitrile.

Acetonitrile is a molecule of symmetry C_{3v}. Absorption is essentially in the VUV, at wavelengths below 182 nm (6.81 eV) [23], where begins a weak continuous band up to about 160 nm (7.74 eV). This is mainly a region of forbidden singlet–triplet transitions [20]. Four allowed singlet–singlet transitions have been observed and analyzed in the 7.9–11.3 eV region, the transitions being π–σ^* n–σ^* and two π–π^* in character. Extensive Rydberg series converging to the 1^2E ground (I.E. = 12.201 eV) and 1^2A_1 first (I.E. = 13.131 eV) excited state of the ion have been analysed in the 8.9–13.2 eV region [20]. Less well-resolved absorption features, observed between 13.2 and 20 eV, are most probably Rydberg bands converging to higher ionization limits. The valence and Rydberg absorption bands of acetonitrile have been assigned or re-assigned recently [20]. The VUV photofragmentation and ionization

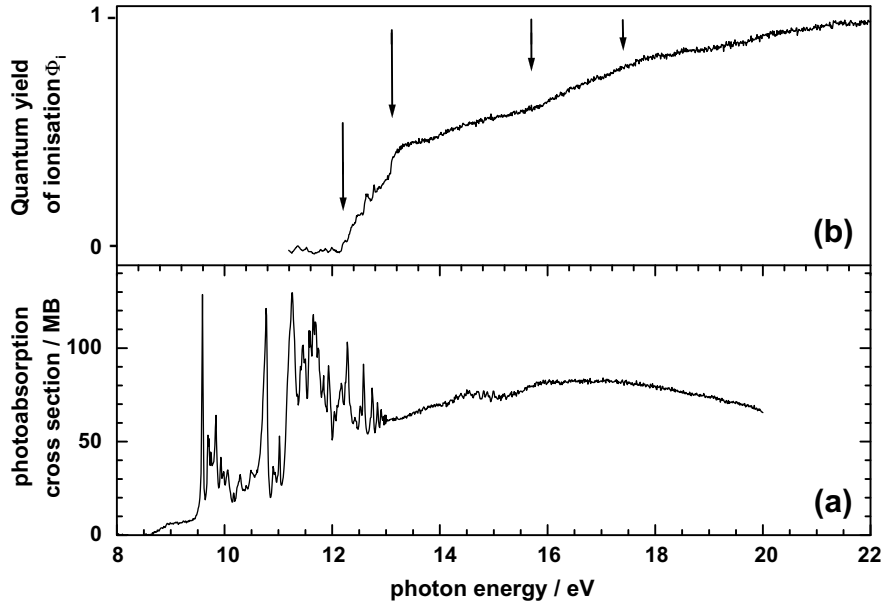

Fig. 1. (a) Absorption spectrum of acetonitrile up to 20 eV; (b) total ionization quantum yield as a function of excitation energy of acetonitrile over the range 11.2–22 eV. Vertical arrows indicate ionization limits.

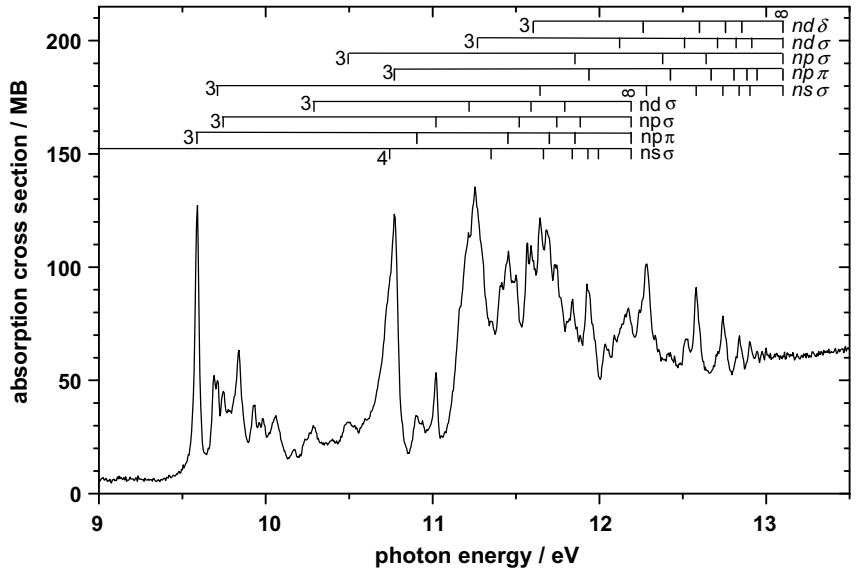

Fig. 2. Absorption spectrum of acetonitrile between 9 and 13 eV.

behaviour will be discussed in Sections 4.1 (fragment fluorescence) and 4.2 (ionization, including dissociative ionization).

4. Results and discussion

4.1. Fluorescence

4.1.1. Dispersed fluorescence spectra

The dispersed fluorescence spectra between 300 and 700 nm obtained at 11.25 and 15 eV photon excitation energies are shown in Fig. 3. At $E_{exc} = 11.25$ eV the observed features are the CN($B^2\Sigma^+ \rightarrow X^2\Sigma^+$) (1,0), (0,0) and (0,1) bands respectively, in the 350–420 nm region, and weak, poorly resolved, CN($A^2\Pi \rightarrow X^2\Sigma^+$) emission in the 500–700 nm region. These same bands are observed at $E_{exc} = 15$ eV and, in addition, the CH ($A^2\Delta \rightarrow X^2\Pi$) (0,0) band is also present in our spectra (Fig. 3). The CN bands were observed at $E_{exc} = 10$, 11 and 13 eV (data not shown). A very weak CH(A-X) band was also observed in the $E_{exc} = 13$ eV fluorescence spectrum. We remark that the dispersed fluorescence spectrum excited at $E = 15$ eV shown in Fig. 3b is the sum of two separate spectra measured under the same conditions on the same day. The resultant spectrum was subjected to a 10 point adjacent averaging smoothing. The apparent two features in the

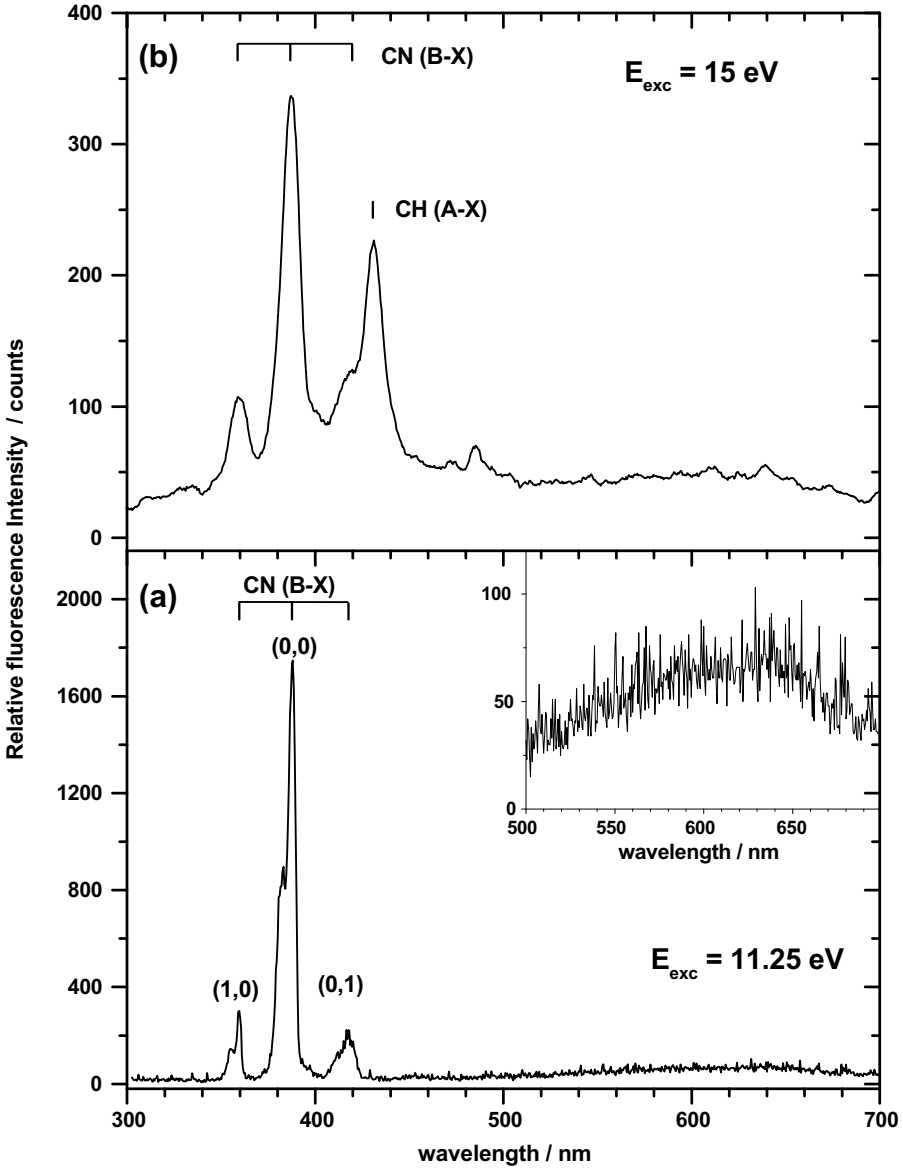

Fig. 3. Dispersed fluorescence spectra between 300 and 700 nm obtained (a) at 11.25 eV photon excitation energy (resolution 4 nm). Insert shows the 500–700 nm region with fluorescence intensity magnified by a factor of 9 and (b) 15 eV photon excitation energy (resolution 10 nm).

480 nm region, and other undulations up to 700 nm, are residual noise. The absence of a strong feature at 656 nm, where a H Balmer-α line would appear, indicates that the more prominent of the two apparent features in the 480 nm region is noise and not due to H Balmer-β emission.

We note that the CH $B^2\Sigma^- \rightarrow X^2\Pi$ (0,0) emission band, whose Q and R heads are at 388.9 and 387.1 nm, respectively, [25], would overlap with the CN(B-X) 0,0 band in the 388 region. From the relative intensities of the CN(B-X) 0,0 and 1,0 bands at $E_{exc} = 11.25$ eV, one can estimate that in the dispersed fluorescence spectrum at $E_{exc} = 15$ eV, which also contains the CH(A-X) 0,0 band, the contribution of the CH(B-X) 0,0 band is very small. This is confirmed by the FEX spectra (see Section 4.1.2).

A further remark is in order, concerning the emission assigned to CN(A-X). A very similar poorly resolved emission in the same spectral region occurs in the VUV photolysis of methane, in which molecule it is due to CH_2(b-a) emission [24]. Although one can conceive of processes forming excited CH_2 by photolysis of acetonitrile, the observation of CN(B-X) bands in our dispersed fluorescence spectra makes it far more likely that the visible region emission is indeed due to CN(A-X) in our case. This argument is strengthened by the fact that in VUV photolysis experiments on CH_3OH and CH_3SH, similar to those they carried out on CH_4, Ma et al. [24] saw CH but detected no CH_2 emission, whereas bands of the dissociation products OH and SH were observed, respectively, these being analogous to our CN emission.

4.1.2. Fluorescence excitation (FEX) spectra

Fig. 4 gives the FEX spectra over the E_{exc} range 8–20 eV, for the CN(A → X) emission at 570 nm, CN(B → X) emission at 388 nm and the CH(A → X) emission at 431 nm. Also shown is an absorption spectrum over this energy range. Measurements of the CN(A-X) FEX spectrum were also made at 600 nm detection.

4.1.2.1. FEX spectra of CN emissions. The CN(A-X) and (B-X) FEX spectra are very similar in their features between 10.8 eV and 14 eV, with some small differences in relative intensities. However, in the 8.0–10.8 eV region the two FEX spectra differ substantially in relative intensities of the salient features. In particular, the strong CN(B-X) FEX band at 9.59 eV, which corresponds to the first strong absorption feature, is very much reduced in relative intensity in the CN(A-X) FEX spectrum. This absorption feature was assigned as the Rydberg band $3p\sigma O_0^0$ by Nuth and Glicker [4] but we have re-assigned it as $3p\pi O_0^0$ [20], in agreement with Gochel-Dupuis et al. [26] and with Eden et al. [2]. The apparent onset for CN(A-X) emission is at 9 ± 0.05 eV, which corresponds to the beginning of the $n \rightarrow \sigma^*$ transition (calculated oscillator strength $f = 0.02$, [20]) although there appear to be some very weak FEX features in the 7–8 eV region, which could correspond to weaker valence transitions observed in the absorption spectrum. An upper limit of 7.21 eV for the CN(A-X) emission threshold energy in acetonitrile has been reported by West and Berry [27]. Excitation below 7.96 eV must be to triplet states of acetonitrile [20]. A number of weak features are observed in the CN(A-X) FEX spectrum between 13.3 and 19 eV. These same features appear, very weakly, in

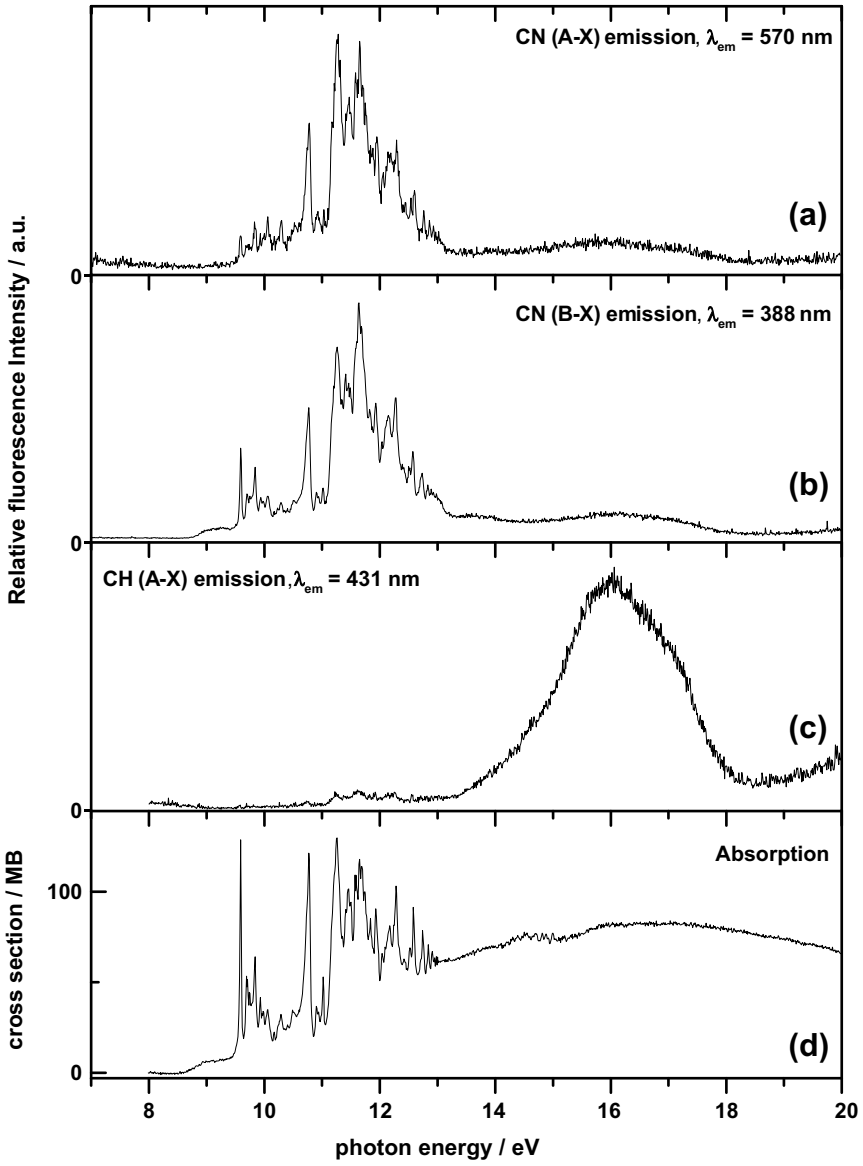

Fig. 4. Fluorescence excitation (FEX) spectra, over the E_{exc} range 8–20 eV for (a) CN(A → X) emission at 570 nm, (b) CN(B → X) emission at 388 nm and (c) CH(A → X) emission at 431 nm, (d) is the absorption spectrum of acetonitrile over this energy range.

the absorption curve and are most probably Rydberg bands converging to the second excited state of the ion at 15.13 eV and to still higher excited states of CH_3CN^+.

Our measured onset of the CN(B-X) emission is at 8.60 ± 0.03 eV. The weak signal then rises featureless to culminate in the strong band at 9.59 eV. This apparently featureless initial region corresponds to a number of weak valence transition vibronic bands in the absorption spectrum, superposed on a background continuum. It is notable that the CN(A-X) FEX spectrum does not contain this band, the first feature being the 9.59 eV Rydberg band which, as stated above, is relatively much weaker than in the CN(B-X) FEX spectrum. We mention that Okabe and Dibeler [7] report the CN(B-X) threshold to be at 8.52 ± 0.03 eV in a FEX spectrum measured over the range 120–150 nm (8.26–10.33 eV) (Our more conservative examination of their Fig. 3 gives the onset at 144.5 nm (8.58 eV).). The FEX spectrum of Okabe and Dibeler shows the same structure as ours although it is slightly less well resolved. An estimated threshold value of 8.53 ± 0.02 eV has also been given, based on the highest populated rotational levels in the CN(B, $v = 0$) state observed over a range of excitation energies [28]. The fluorescence quantum yield of CN(B-X) emission, which has been measured in the 9–13 eV interval [6] has a reported maximum value of 1.9% in the region of the strongest absorption band at 11.26 eV, which is the region of the $3^1A_1 \rightarrow 1^1A_1O_0^0$ valence transition band and the O_0^0 band of the 3dσ Rydberg series converging to the first excited state of the ion [20]. Using our measured absorption cross sections (Fig. 1a) [20], which are 20% higher than those of Suto and Lee [30], we revise this maximum fluorescence yield value to 1.5%. We note that the ratio of the fluorescence intensities of CN(A-X) to CN(B-X) is reported to be of the order of 0.3 over most of the excitation interval 8.6–11.7 eV [3]. Our quantitative measurements of FEX intensities confirm this value.

In the energy region above 14.5 eV, both CN(A-X) and (B-X) emissions rise slowly to a maximum in the 16 eV region, then decline to a quasi-plateau between 18 eV and our measurement upper limit, 20 eV, with a slight rise in intensity above 19 eV. Kanda et al. [6] observed, in their CN(B-X) and CN(A-X) emission cross sections, a maximum at ≈16 eV, followed by a minimum at ≈19 eV and a further rise to a maximum at ≈22.3 eV. The fluorescence yields of CN(B-X) and CN(A-X) at 16 eV we estimate to be of the order of 0.2% and 0.07%, respectively.

4.1.2.2. FEX spectra of CH emission. The CH(A-X) FEX spectrum has a few weak features in the 10–13 eV region that apparently correspond to features in the absorption spectrum. Although they could be intrinsic to CH emission it is more probable that these FEX features are due to partial overlap of CH A-X (0, 0) band emission with the CN B-X (0, 1) band at 422 nm. This is supported by the fact that only CN emission, and never any CH emission, has been reported in VUV induced fluorescence experiments on acetonitrile at excitation energies below 11.7 eV [3,7,28,29]. We consider that the intrinsic CH(A-X) emission onset energy is 13.34 ± 0.03 eV, followed by a peak at about 16.0 eV. Ours is the first report of CH emission induced by photolysis of acetonitrile, presumably because our study is the first in which photon excitation exceeded 11.7 eV in energy.

Possible reactions forming CH(A) are discussed later, after an initial discussion of the formation of excited CN molecules. We note that from the observed CH(A-X) onset energy one can estimate that the CH(B-X) onset energy would be at 13.65 eV, and that the corresponding signal should rise sharply at higher energies. As stated previously, the CH B-X (0, 0) band would overlap with the CN(B-X) band at 388 nm. Examination of the FEX spectrum of the 388 nm band shows very little modification in the signal in the 13.65 eV excitation energy region, thus confirming that the contribution of the CH(B-X) emission to the 388 nm fluorescence signal is very small.

4.1.3. Interpretation of FEX spectra

The close resemblance between the CN FEX spectra and the absorption spectrum of acetonitrile indicates that the relevant valence and Rydberg levels of CH_3CN are coupled directly or indirectly to dissociative continua.

We estimate the thermochemical threshold for the reaction

$$CH_3CN + h\nu \rightarrow CH_3(^2A_2'') + CN(B^2\Sigma^+), \quad (1)$$

to be 8.54 eV. This is in a region of weak vibronic valence bands and it is close to the energy of the origin band of the π–π^* $2^1E - 1^1A_1$ valence transition at 8.45 eV [20]. It is also close to measured onset values. We note that electronic transitions in acetonitrile, whether valence or Rydberg, are allowed only to excited electronic states of $^1A_1$ and ^1E symmetries. In order for the acetonitrile dissociation products to be $CH_3(^2A_2'') + CN(B^2\Sigma^+)$, where CH_3 is formed in its ground electronic state $^2A_2''$, application of the Wigner–Witmer correlation rules [23] indicates that the dissociative electronic state should have electronic or vibronic symmetry A_1.

$$CH_3CN(^1A_1) \rightarrow CH_3(^2A_2'') + CN(B^2\Sigma^+) \quad (2)$$

A vibronic dissociation pathway is not unlikely since fragmentation from a ^1E electronic state to give $CN(B^2\Sigma^+)$ would lead to CH_3 being formed in an excited state [23]. We note, however, formation of $CN(A^2\Pi)$ and $CH_3(^2A_2'')$ can occur by dissociation of an excited ^1E state,

$$CH_3CN(^1E) \rightarrow CH_3(^2A_2'') + CN(A^2\Pi). \quad (3)$$

and that intramolecular rovibronic coupling exists between $CN(B^2\Sigma^+)$ and $CN(A^2\Pi)$ electronic states [30]. This provides another, more indirect, pathway for forming $CN(B^2\Sigma^+)$ and ground state CH_3 from an acetonitrile ^1E state.

The thermochemical threshold of CN(A) appearance is calculated to be at 6.386 eV. A triplet state of acetonitrile has been reported in this energy region [31], in agreement with our triplet state calculations [20]. This is below the initial energy of our FEX measurements. The absence of a CN(A-X) signal in the 9 eV region indicates that coupling of the excited CH_3CN state to the $CH_3(^2A_2'') + CN(A^2\Pi)$ dissociation continuum is weak in this energy region. However, absorption to Rydberg levels at and above 9.59 eV ($3p\pi$) appears to excite levels which couple to both the $CH_3 + CN(B)$ and $CH_3 + CN(A)$ dissociation continua, but whose branching ratios vary with excitation energy (Fig. 4).

We remark that a competitive dissociation reaction can also occur, as has been determined for 10.2 eV photon excitation by Moriyama et al. [32]. This is the H loss reaction, occurring mainly via the process:

$$CH_3CN(^1A_1) + h\nu \rightarrow CH_2CN + H. \quad (4)$$

This reaction has a thermochemical onset value of 4.031 eV and it has been observed with 184.9 nm (6.7 eV) irradiation [33], at which energy it dominates over the carbon–carbon rupture process. The H-loss reaction is considered to be the major photodissociation channel in the VUV region [6]. In dissociative ionization, the loss of a H atom is preceded by isomeric conversion [34]. It is not known whether a similar isomeric conversion occurs for H-loss in neutral photodissociation.

The thermochemical threshold for the formation of H(2s,2p) is 14.23 eV. For H (Balmer-α) it is 16.12 eV, which is above the highest excitation energy (16 eV) in our dispersed fluorescence measurements. Excited H emissions have not been looked for in studies on acetonitrile photodissociation.

Two possible reaction channels were considered for the formation of CH(A). These are:

$$CH_3CN + h\nu \rightarrow CH(A) + H + HCN. \quad (5)$$

and

$$CH_3CN + h\nu \rightarrow CH(A) + H_2 + CN(X). \quad (6)$$

Reaction (5) has a thermochemical onset energy of 11.927 eV, and reaction (6) of 12.777 eV. These values are sensibly less than the observed onset for CH(A-X) emission, so that a reaction barrier could exist; complex reaction pathways may be involved at and above the 13.34 eV onset. The initial stage of the reaction is probably the H atom loss reaction (4). At 10.2 eV photon excitation (to the $n = 3$ Rydberg levels) the formation of CH_2CN is considered to occur via internal conversion of the excited molecule to the ground state of acetonitrile [32]. CH_2CN would have to be created with a much greater internal energy in reaction (6) than in the more favoured reaction (5). Whether coupling to the ground state potential energy surface also occurs at the photon excitation energies corresponding to the CH(A-X) FEX signal is not known. We hope that our results will encourage the elaboration of potential energy surfaces by quantum chemistry calculations so as to further understand the various dissociation pathways discussed in the present study.

4.2. Ionization

Our measurements of total ionization enabled us to determine the quantum yield of photoionization as a function of excitation energy. Photoion curves of parent and fragment ions have been measured by several authors over the 12–20 eV energy region [5,35]. The spectrally well resolved photoion curves of the parent ion and the H-loss fragment ion measured by Rider et al. [5] exhibit features that we can compare with those of our absorption spectra, as discussed below. We first present and discuss our photoionization quantum yield measurements.

4.2.1. Photoionization quantum yields

No previous measurements of the photoionization quantum yields of acetonitrile have been reported. Fig. 1 gives the total ionization yield as a function of excitation energy over the range 11.2–22 eV, compared with the absorption curve up to 20 eV. The ionization onset, at 12.22 ± 0.02 eV, is in excellent agreement with the known ionization energy of acetonitrile, 12.201 ± 0.002 eV determined by photoelectron spectroscopy [36]. This ionization corresponds to loss of a π(CN) electron in the 2e molecular orbital [20]. The ionization yield curve contains structure up to 13.1 eV, the second ionization limit (1^2A_1 state), where there is loss of a n_N electron from the $7a_1$ M.O. [36]. At this energy, the total ionization yield $\Phi(i) = 0.39$, rising steeply to $\Phi(i) = 0.46$ immediately after this threshold for formation of the 1^2A_1 state. There are no marked discontinuities in the absorption curve at this energy. The features in the ionization yield curve up to about 14 eV are the same as those for the parent ion yield curve [5] (see Section 4.2.2). The latter falls off after 14.5 eV. The rise in the total ionization yield curve above 14.5 eV, with a slight change of slope at the third ionization limit at 15.1 eV (2^2E), is due to the contribution of fragment ions, the lowest of whose appearance energies is 13.94 eV ($C_2H_2N^+$) [37]. Other fragments produced by dissociative ionization of acetonitrile have threshold energies in the range 15.25–15.56 eV, which is a region of excitation to vibronic levels of the second excited state of the ion, whose vertical I.E. = 15.133 eV. There is a slight, rising, change of slope at 15.13 eV in the total ionization yield curve (Fig. 1b), more marked in the absorption curve (Fig. 1a).

Some very diffuse structures exist in the ionization yield curve, e.g., at 15.7 eV. The yield curve reaches a plateau at 21.3 eV, where $\Phi(i) = 1$. This is about 9.14 eV above the first ionization energy. It is interesting that this energy difference between ionization onset and the energy at which $\Phi(i) = 1$ is similar to that for polycyclic aromatic hydrocarbons, which led us in the past to suggest a rule of thumb for determining the energy at which the ionization yield is unity for these aromatic species [22,38].

It is of interest that in a photoion-fluorescence photon coincidence (PIFCO) measurement on acetonitrile with HeI 58.4 nm (21.21 eV) radiation, fluorescence emission of CN(B-X) was observed which arose from a neutral dissociation channel and not in coincidence with an ion product [39]. If this surprising observation is confirmed, and is not due to excitation by lower energy lines present in the helium lamp emission, then a neutral dissociation channel exists in acetonitrile at an energy just below that where $\Phi(i) = 1$. A CN(B-X) fluorescence quantum yield at 21.21 eV associated with neutral dissociation must have a value of the order of 1% or less. The CN(B-X) emission observed by Kanda et al. above 22 eV [6] most probably arises from a dissociative ionization process, but this remains to be tested.

4.2.2. Comparison of parent and fragment photoion yield curves with absorption and other spectra

Two spectral regions are of particular interest for a comparison between the photoion yield curves and the photoabsorption spectrum, (i) the 12.28 and 13.01 eV region, and (ii) the 14.212–15.1 eV region.

4.2.2.1. 12.28–13.01 eV region. The vibronic absorption peaks between 12.28 and 13.01 eV (Figs. 1a and 2) are also observed in the parent ion yield curve [5]. Table 2 gives our absorption peak energies compared with those reported for the parent ion yield curve (Fig. 3 of Rider et al. [5]). These peaks correspond to Rydberg bands converging to the first excited state of the ion. Rider et al assigned the peaks in this energy region to a series of nsσ bands ($n = 6$–12; $n = 11$ not observed) and to two ndδ bands ($n = 5$ and 6). We agree with their assignments for the 6dδ band and for the $n = 6$–9 bands of the nsσ series. Differences in assignment occur for three of the bands of Rider et al. given in our Table 2, where we report the energies and our assignments of absorption bands close to the peak energies given by Rider et al. The differences between our peak energies and those reported by Rider et al may be due to differences in energy calibration but also, more probably, to the existence of overlapping unresolved features in the parent ion yield curve.

Table 2
Absorption and FEX peak energies[a] of acetonitrile compared with those reported by Rider et al. [5] for the parent ion yield curve in the 12.28–13.01 eV region

Photoion [5] eV (α)	Assign.[a] [5]	Absorption present study eV (β)	Assign.[a] present study	(α) − (β) meV	FEX eV CN(B-X)
12.601	6sσ	12.580	$6s\sigma O_0^0$	21	12.58
		12.600	$5d\delta O_0^0$	1	
12.775	7sσ	12.740	$7s\sigma O_0^0$	35	12.73
		12.756	$6d\delta O_0^0$	19	
12.864	8sσ	12.838	$8s\sigma O_0^0$	26	12.84
		12.854	$7d\delta O_0^0$	10	
12.924	9sσ	12.903	9sσ	21	
		12.914	$8d\sigma O_0^0$	10	
12.964	10sσ	12.945	$9p\pi O_0^0$	21	
		12.976	$7p\pi 3_0^1$	−12	
13.020	12sσ	13.010	$7d\delta 3_0^1$	10	13.0
12.542	5dδ	12.528	$5p\pi 4_0^1$	14	12.52
		12.580	$6s\sigma O_0^0$	−38	
12.724	6dδ	12.708	$6d\delta O_0^0$	16	12.73
		12.740	$7s\sigma O_0^0$	−16	

[a] Rydberg states converging to the first excited state 1^2A_1 of the acetonitrile ion.

The parent ion yield features in the 12.28–13.01 eV region also occur in the CN(A-X) and CN(B-X) FEX spectra. The peak energies of the CN(B-X) FEX bands are reported in Table 2. They agree satisfactorily, within the respective error limits, with the ion yield and absorption peak energies. Photoionization and photodissociation are competitive processes for relaxation of the excited levels in this energy region.

4.2.2.2. 13.5–20 eV region. The ions produced by photon excitation between 13.5 and 15.1 eV are formed by autoionization since this is a region of zero signal in HeI photoelectron spectra of acetonitrile [36]. Features in the parent ion and $C_2H_2N^+$ fragment photoion yield curves of CH_3CN, observed by Rider et al. [5] in the 14.212–15.4 eV region, are present in our total ionization yield curves, and they also occur in the acetonitrile absorption spectrum [20] where we observe a set of bands between 13.9 and 15.5 eV and some weaker features, barely above the noise level, overlying a broad continuum between 15.13 and 20 eV. We have interpreted [20] these absorption bands as vibronic features belonging to a 4d Rydberg series converging to the second excited state of the ion, 2^2E at 15.133 ± 0.002 eV [36], with a quantum defect $\delta = 0.16$. The broad absorption feature mentioned above begins at about 15.1 eV. The assignment of the bands in the 13.9–15.5 eV region is confirmed by the good match between these absorption features and the most intense of the vibronic features of the third photoelectron band in the HeI photoelectron spectrum [36,40], between 15.1 and 16 eV, corresponding to the formation of the origin level at 15.133 ± 0.002 eV and to vibrational components of the second excited electronic state of the acetonitrile ion [20]. The absorption features lie about 0.92 eV below the corresponding PES features.

Our 4d series assignment differs from that of Rider et al. [5]. They assigned the ion yield features in the 14.212–15.1 eV region to vibronic components of the nsσ (i.e., nsa_1) Rydberg levels, beginning with the $n = 5s\sigma$ level at 14.212 eV, converging to this second excited electronic state of the acetonitrile ion. Their reported average quantum defect of 1.06 was based on the PES analysis of Turner et al [40] who gave 15.2 eV as the ion state energy. As stated above, our analysis of the absorption spectrum in this energy region has led us to assign the Rydberg series as 4d, with a quantum defect of 0.16 [20], with the 14.212 eV band as its origin.

The photoion peak energies in this spectral region were not given in the publication of Rider et al. [5], but

presented graphically in their Fig. 4. A direct comparison of our absorption spectrum and this parent photoion curve, at the same energy scale, shows convincingly that the two spectra have features at the same energies. The weakness and relatively poor resolution of the absorption and ion yield features in the 14–15.3 eV region make it difficult to propose definite transition assignments, including vibrational components, for these features. However, the good match between the absorption spectrum in the 14.212–15.8 eV region and the third band of the photoelectron spectra suggests that modes 3 and 4 are the most prominently excited vibrations, as components of the Rydberg states in this part of the absorption spectrum, with frequencies $\nu_3 \approx 180$ meV and $\nu_4 \approx 100$ meV as determined from the PES and discussed elsewhere [20].

We note that the corresponding features between 14.212 and 15.332 eV are not observed in the ion yield curves of CD_3CN [5]. The Rydberg levels are subject to autoionization as well as predissociation, the latter probably via crossing to dissociative potential energy surfaces. The branching ratio for ionization and dissociation is therefore different for CH_3CN and CD_3CN in this spectral region, illustrating an interesting isotope effect.

5. Astrophysical implications

The results of our spectroscopic and photophysical studies on acetonitrile have implications in astrophysics in several areas discussed below: the interstellar medium, comets and planetary atmospheres. Acetonitrile is considered to be one of the building blocks of life [9]. If synthesized and preserved during the formation of the solar nebula, it could be transported to Earth via asteroids, comets and meteors, all of which vectors can provide protective environments.

5.1. Interstellar medium

In H I regions of the interstellar medium (ISM) the upper limit energy of radiation (E) is 13.6 eV. In these regions subject to UV and VUV radiation, but where $E \leqslant 13.6$ eV, acetonitrile would undergo neutral photodissociation and, between 12.2 and 13.6 eV, parent ion formation, but not ion fragmentation. The dissociative photoionization onset (H-loss channel), at 13.94 eV, is above the H I limit. The photoionization quantum yield of acetonitrile at 13.6 eV is 0.53 (Fig. 1b). Taking into account our measured VUV absorption cross sections, we have revised the calculations of Suto and Lee [3] on the integrated photodissociation rate of acetonitrile in the 6.89–10.78 eV (115–180 nm) region due to the interstellar radiation field in the solar neighbourhood. Our value for this photodissociation rate is $2.7 \times 10^{-9}\ s^{-1}$.

Protection from the destructive effects of VUV radiation is necessary for detectable amounts of acetonitrile to exist in the ISM. Neutral acetonitrile has been observed towards protostars [41,42], in particular in hot molecular cores [43], which are warm condensations inside molecular clouds associated with active star formation regions, whose density is such that they will offer molecules some protection against radiation. Much attention has been paid to acetonitrile associated with ultracompact H II regions [44], which are found, possibly clumpy, within dense molecular cores whose radii are in the 0.01–0.6 pc range [45–47]. The CH_3CN molecules in massive star-formation regions tend to be in a compact region (10^4–10^5 AU) [46], with temperatures in the 100–200 K range. It is thought that the molecule occurs in a dense shell which forms behind a shock and in front of an ionization front, creating a marginal shell to the Strömgren sphere formed by photoionization of hydrogen atoms. A typical ultracompact H II region occurs in G $34.3 + 0.15$, where CH_3CN is observed [47]. The molecule has been suggested to be synthesized on dust grain surfaces and injected into the ISM by evaporation or by shocks, but this is found not to account for observed abundances [48]. Mackay [49] has proposed that acetonitrile is formed by gas phase reactions, mainly via the radiative association reaction of CH_3^+ with HCN to form CH_4CN^+, followed by dissociative recombination with electrons to form $CH_3CN + H$. Another possible route is via radiative association of the two neutral species $CH_3 + CN$.

The photodestruction pathway of CH_3CN proposed in all astrophysical situations [49] has been $CH_3CN \rightarrow CH_3 + CN$. However, the major photodissociation pathway in the VUV is $CH_3CN \rightarrow CH_2CN + H$ [6] as discussed in Section 4.1.2. Appropriate modification of models involving photodestruction of CH_3CN is thus required, especially since it appears that photodestruction rates used at present are often really arbitrary estimates [50–53]. We remark that in certain sites, other processes of destruction of CH_3CN can occur, such as by reaction with ions, C^+, H_3^+, H_3O^+, as is suggested to be the case within the densest part of dark cloud cores [54].

Another source of CH_3CN is in protoplanetary discs around young stars [51], where most of the radiation flux is Lyman-α. The stellar radiation field can differ considerably from that of the standard interstellar radiation field, especially for the cooler T Tauri stars. The UV field can be several orders of magnitude greater than the field usually considered to exist in studies on molecular clouds. Van Dishoek et al. [51] remark that with such high fluxes, the rates of photodestruction can become comparable to the rates of dissociative recombination, so that the photodissociation of ions, of which little is known experimentally, should be included in model schemes. In general, since stellar VUV spectral intensities and their distributions depend on the type of source star illuminating a gaseous medium, this has to be taken into account in modelling irradiation effects using the absorption spectrum of acetonitrile.

We remark that, besides direct ionization events, a UV field can occur via the emission of X-rays by young stars, due to the formation of secondary electrons and their interaction with molecular hydrogen, giving rise to H_2VUV emission [51]. It is also important to note that in young

stars, the H Lyman-α flux can be 10 times greater than at the present day [55]. These conditions should be taken into account in modelling the chemistry of acetonitrile at those epochs, using the VUV spectroscopic and photophysical properties of CH_3CN.

5.2. Comets

Acetonitrile has been observed in comets [14,15] both by radiofrequency and by mass spectroscopies [56]. Its release on the Deep Impact encounter with comet 9P/Tempel 1, has been suggested by I.R. emission observations [15]. Its abundance, e.g., in comet Hale–Bopp is 0.02% of that of H_2O [57]. CN(B-X) emission is commonly observed early as a comet approaches the sun. One mechanism for formation of CN(B) is solar photodissociation of parent molecules, amongst which is CH_3CN, for which we find the CN(B-X) fluorescence quantum yield $\sigma(F) \leqslant 1.5\%$. Modellers consider that CN(X), which could be excited to the CN(B) state by solar radiation, is not formed by VUV photodissociation of CH_3CN [58,59]. This assertion is based on the experimental results of Halpern and Tang [60], who photolysed acetonitrile at 158 nm (7.847 eV). Our absorption spectral analysis [20] shows that the electronic state excited at 158 nm indeed cannot dissociate to CN(X) but that such a dissociation could occur at other energies. Thus this channel is not to be excluded without further laboratory studies.

5.3. Planetary atmospheres and the ISM

The photodissociation rate of acetonitrile is required for model calculations of acetonitrile formation and destruction in the stratosphere, in the atmosphere of Titan, as well as for calculation of acetonitrile destruction in the ISM. For the atmosphere of Titan it is necessary to take into account the latitude since, e.g., at the time of the Voyager flyby (1980), the tilt of Titan's axis of rotation limited the amount of solar UV and VUV reaching its atmosphere at latitudes higher than 70° north [61].

We have revised the calculations carried out by Suto and Lee [3], taking into account our measured VUV absorption cross sections. We find that the integrated absorption over the 106–180 nm region is 1390 mB. This is used to determine the integrated photodissociation rate by the solar flux (over 115–180 nm) on the top of the Earth's atmosphere (altitude 266 km, solar flux measurements May 17, 1982 [62]), which is found to be $10^{-5}\,s^{-1}$. The contribution of solar Lyman-α is about 85% (but we remark that Lyman-α intensity can vary by a two-fold factor over a present-day solar cycle [63]). The photodissociation rate of CH_3CN is negligibly small in the troposphere and the stratosphere, due to screening by O_2, CO_2 and H_2O. In these sites the destruction of CH_3CN is essentially due to chemical reactions with OH, $O(^1D)$ and other species [64]. The reaction rate of CH_3CN with OH is of the order of $10^{-7}\,s^{-1}$ in the stratosphere. Thus one can conclude that, on Earth, photodissociation by the solar flux would be the dominant destruction channel of acetonitrile only above an altitude of 50 or 60 km.

We note that our value for the integrated photodissociation rate, $2.7 \times 10^{-9}\,s^{-1}$, due to the interstellar radiation field in the solar neighbourhood is very small as compared with that due to the solar flux on top of the atmosphere, as well as the $\approx 10^{-7}\,s^{-1}$ rate due to the solar flux at Titan.

5.4. Further remarks

(i) Interstellar and atmospheric model calculations involving the VUV must take into account the variation of the photoionization yield, measured here for the first time for acetonitrile, in the 10 eV interval above the ionization energy.

(ii) With respect to solar, stellar or interstellar radiation fields, we remark that H Ly-α, at 121.5 nm, is below the ionization limit of acetonitrile, whereas at the HeI emission energy at 58.4 nm, the quantum yield of ionization is unity.

(iii) A study of the lifetime of acetonitrile during UV photolysis, related to its survival in space, has been made by Bernstein et al. [65]. They irradiated a film of CH_3CN at 15 K, as well as in argon and water matrices at 15 K, with a hydrogen lamp producing photons essentially between 7.75 and 10.2 eV. From a measure of the rate of disappearance of the acetonitrile I.R. absorption under these conditions, they estimated the half-life of acetonitrile in the diffuse interstellar medium (≈1000 years) and in solar system ices (weeks on upper surface of Europa). These values relate to integrated photolysis effects over only the 7.75–10.2 eV excitation range. They do not take into account the effects of VUV radiation above 10.2 eV, which would include ionization at and above 12.201 eV. Furthermore, the rates and half-lives are certainly dependent on solid state effects and on the chemical nature of the matrix. It is thus somewhat illusory to extrapolate the acetonitrile photodestruction rates of Bernstein et al. [65] to the gas phase relevant in cometary, atmospheric and interstellar sites.

6. Conclusion

In the present study on the VUV photophysics of acetonitrile we carried out the following measurements, using monochromatised synchrotron radiation as the photon excitation source: (1) the dispersed fluorescence spectra between 250 and 700 nm excited at various photon excitation energies between 10 and 16 eV; (2) fluorescence excitation (FEX) spectra for emission bands of CN(B-X) and (A-X) transitions and, for the first time, of CH(A-X), over the photon excitation range 8–20 eV; (3) the photoionization quantum yield between 11 and 22 eV, never previously measured for acetonitrile.

The CN FEX observations follow closely the absorption spectrum, with some differences reflecting the branching ratios for forming the $CN(A^2\Pi)$ and $CN(B^2\Sigma^+)$ states. The quantum yields of CN fluorescence are less than 2% over the whole excitation energy range explored. $CH(A^2\Delta \rightarrow X^2\Pi)$ emission appears to be mainly associated with the continuous background absorption of acetonitrile above 13.3 eV. The formation of the CN and CH excited states is discussed in terms of photodissociation processes involving acetonitrile excited states of specific electronic and vibronic symmetries. Structure in the total and partial photoionization yield curves is discussed with respect to features observed in the absorption spectrum of acetonitrile, and their Rydberg band assignments.

The absorption and photophysical study results on acetonitrile have implications in several areas of astrophysics: the interstellar medium, in particular concerning effects of the interstellar and various stellar or proto-stellar radiation fields on the photodestruction of CH_3CN; comets, where it is shown that the acetonitrile photodissociation mechanisms used in modelling are incomplete; planetary atmospheres, including the Earth's, for which the photodissociation rates of acetonitrile by the solar flux are compared with rates of chemical reactions destroying acetonitrile. The information provided by the photoionization quantum yields as a function of excitation energy is shown to be of potential use in cosmochemical modelling.

Acknowledgements

We acknowledge support from the European Commission programme "Access to Research Infrastructures" for providing access to the Berlin BESSY synchrotron under contract FMRX-CT-0126. We thank the CNRS Groupe de Recherche "GDR Exobiologie" (GDR 1877) for support of this work.

References

[1] R.S. Berry, S. Leach, Adv. Electron. Electron. Phys. 57 (1981) 1.
[2] S. Eden, P. Limão-Vieira, P. Kendall, N.J. Mason, S.V. Hoffmann, S.M. Spyrou, Eur. Phys. J. D26 (2003) 201.
[3] M. Suto, L.C. Lee, J. Geophys. Res. 90 (1985) 13037.
[4] J.A. Nuth, S. Glicker, J. Quant. Spectrosc. Rad. Transfer 28 (1982) 223.
[5] D.M. Rider, G.W. Ray, E.J. Darland, G.E. Leroi, J. Chem. Phys. 74 (1981) 1652.
[6] K. Kanda, T. Nagata, T. Ibuki, Chem. Phys. 243 (1999) 89.
[7] H. Okabe, V.H. Dibeler, J. Chem. Phys. 59 (1973) 2430.
[8] H. Neuimin, A. Terenin, Acta Physicochim. U.R.S.S. 5 (1936) 465.
[9] A. Brack (Ed.), The Molecular Origins of Life, Cambridge Univ. Press, Cambridge, UK, 1998.
[10] P.M. Solomon, K.B. Jefferts, A.A. Penzias, R.W. Wilson, ApJ 168 (1971) L107.
[11] B.L. Ulich, E.K. Conkling, Nature 248 (1974) 121.
[12] M.T. Beltran, R. Cesaroni, C. Codella, L. Testi, R.S. Furuya, L. Olmi, Nature 443 (2006) 427.
[13] L.E. Snyder, D. Buhl, ApJ 163 (1971) L47.
[14] W.B. Huebner, L.E. Snyder, D. Buhl, Icarus 23 (1974) 580.
[15] M.F. A'Hearn, M.J.S. Belton, W.A. Delamere, J. Kissel, et al., Science 310 (2005) 258.
[16] L.M. Lara, E. Lellouch, J.J. López-Moreno, R. Rodrigo, J. Geophys. Res. 101 (1996) 23261.
[17] A. Marten, T. Hidayat, Y. Biraud, R. Moreno, Icarus 158 (2002) 532.
[18] E. Arijis, D. Nevejans, J. Ingels, Int. J. Mass Spectrom. Ion Proc. 81 (1987) 15.
[19] K.H. Becker, A. Ionescu, Geophys. Res. Lett. 9 (1982) 1349.
[20] S. Leach, M. Schwell, S. Un, H.W. Jochims, H. Baumgärtel, this issue, doi:10.1016/j.chem.phys.2007.12.012.
[21] M. Schwell, F. Dulieu, H.W. Jochims, J.L. Chotin, H. Baumgärtel, S. Leach, in: Frontiers of LifeProc. Xth Rencontres de Blois (2000), The Goioi Publishers, Vietmam, 2003, p. 53.
[22] H.W. Jochims, H. Baumgärtel, S. Leach, Astron. Astrophys. 314 (1996) 1003.
[23] G. Herzberg, Molecular Spectra and Molecular Structure III. Electronic Spectra and Electronic Structure of Polyatomic Molecules, van Nostrand Reinhold, New York, 1966.
[24] G. Ma, M. Suto, L.C. Lee, J. Quant. Spectrosc. Rad. Transfer 44 (1990) 379.
[25] R.W.B. Pearse, A.G. Gaydon, The Identification of Molecular Spectra, third ed., Chapman and Hall, London, 1965.
[26] M. Gochel-Dupuis, J. Delwiche, M.-J. Hubin-Franskin, J.E. Collin, F. Edard, M. Tronc, J. Am. Chem. Soc. 112 (1990) 5425.
[27] G.A. West, M.J. Berry, J. Chem. Phys. 61 (1974) 4700.
[28] M.N.R. Ashfold, J.P. Simons, J. Chem. Soc., Faraday Trans. II 74 (1978) 1263.
[29] M. Moriyama, Y. Tsutsui, K. Honma, J. Chem. Phys. 108 (1998) 6215.
[30] S. Leach, Can. J. Chem. 82 (2004) 730.
[31] R. Rianda, R.P. Frueholz, A. Kuppermann, J. Chem. Phys. 80 (1984) 4035.
[32] M. Moriyama, Y. Tsutsui, K. Honma, J. Chem. Phys. 108 (1998) 6215.
[33] D.E. McElcheran, M.H.J. Wijnen, E.W.R. Steacie, Can. J. Chem. 36 (1958) 321.
[34] J.C. Choe, Int. J. Mass Spectrom. 235 (2004) 15.
[35] V.H. Dibeler, S.K. Liston, J. Chem. Phys. 48 (1968) 4765.
[36] M. Gochel-Dupuis, J. Delwiche, M.-J. Hubin-Franskin, J.E. Collin, Chem. Phys. Lett. 193 (1992) 41.
[37] J.L. Holmes, F.P. Lossing, P.M. Mayer, Chem. Phys. Lett. 212 (1991) 134.
[38] S. Leach, Zeits. f. Phys. Chem. 195 (1996) 15.
[39] R.C. Dunbar, D.W. Turner, J. Chem. Soc., Faraday II 76 (1980) 1079.
[40] D.W. Turner, C. Baker, A.D. Baker, C.R. Brundle, Molecular Photoelectron Spectroscopy, Wiley-Interscience, London, 1970.
[41] S.V. Kalenskii, V.G. Promislov, A.V. Alakoz, A. Winnberg, L.E.B. Johansson, Astron. Astrophys. 354 (2000) 1036.
[42] V. Pankonin, E. Churchwell, C. Watson, J.H. Bieging, Astrophys. J. 558 (2001) 194.
[43] E. Araya, P. Hofner, S. Kurtz, L. Bronfman, S. DeDeo, Astrophys. J. Suppl. Ser. 157 (2005) 279.
[44] C.R. Purcell, R. Balasubramanyam, M.G. Burton, A.J. Walsh, V. Minier, et al., Mon. Not. R. Astron. Soc. 367 (2006) 553.
[45] R.L. Akeson, J.E. Carlstrom, Astrophys. J. 470 (1996) 528.
[46] C. Watson, E. Churchwell, V. Pankonin, J.H. Bieging, Astrophys. J. 577 (2002) 260.
[47] L. Olmi, R. Cesaroni, P. Hofner, S. Kurtz, E. Churchwell, C.M. Walmsley, Astron. Astrophys. 407 (2003) 225.
[48] T.J. Millar, G.H. MacDonald, A.G. Gibb, Astron. Astrophys. 325 (1997) 1163.
[49] D.D.S. Mackay, Mon. Not. R. Astron. Soc. 304 (1999) 61.
[50] E.F. van Dishoek, in: T.J. Millar, D.A. Williams (Eds.), Rate Coefficients in Astrochemistry, Kluwer, Dordrecht, 1988, p. 49.
[51] E.F. van Dishoek, B. Jonkheid, M.C. van Hemert, Faraday Discuss. 133 (2006) 231.
[52] R. Gredel, S. Lepp, A. Dalgarno, E. Herbst, Astrophys. J. 347 (1989) 289.

[53] W.G. Roberge, D. Jones, S. Lepp, A. Dalgarno, Astrophys. J. Suppl. Ser. 77 (1991) 287.
[54] L.A.M. Nejad, R. Wegenblast, Astron. Astrophys. 350 (1999) 204.
[55] T. Penz, H. Lammer, Yu.N. Kilikov, H.K. Biernat, Adv. Space Res. 36 (2005) 241.
[56] J. Crovisier, Faraday Discuss. 133 (2006) 375.
[57] D. Bockelée-Morvan, D.C. Lis, J.E. Wink, D. Despois, J. Crovisier, et al., Astron. Astrophys. 353 (2000) 1101.
[58] V.A. Krasnopolsky, Astron. Astrophys. 245 (1991) 310.
[59] N. Fray, Y. Bénilan, H. Cottin, M.-C. Gazeau, J. Crovisier, Planet. Space Sci. 53 (2005) 1243.
[60] J.B. Halpern, X. Tang, Chem. Phys. Lett. 122 (1985) 294.
[61] D.W. Clarke, J. Ferris, Origins Life Evol. Biosphere 27 (1997) 225.
[62] G.H. Mount, G.J. Rottman, J. Geophys. Res. 88 (1982) 5403.
[63] D.M. Hunten, J.-C. Gérard, L.M. François, in: The Sun in Time, 1991, pp. 463–497.
[64] G. Brasseur, R. Zellner, A. De Rudder, E. Arjis, Geophys. Rev. Lett. 12 (1985) 117.
[65] M.P. Bernstein, S.F.M. Ashbourn, S.A. Sandford, L.J. Allamandola, Astrophys. J. 601 (2004) 365.
[66] NIST Chemistry Webbook (June 2005), National Institute of Standards and Technology Reference Database. Available from <http://webbook.nist.gov>.
[67] K.P. Huber, G. Herzberg, Molecular Spectra and Molecular Structure IV. Constants of Diatomic Molecules, van Nostrand Reinhold, New York, 1979.
[68] S.G. Lias, J.E. Bartmess, J.F. Liebmann, J.L. Holmes, R.D. Levin, W.G. Mallard, J. Phys. Chem. Ref. Data 17 (Suppl. 1) (1988).